Communication

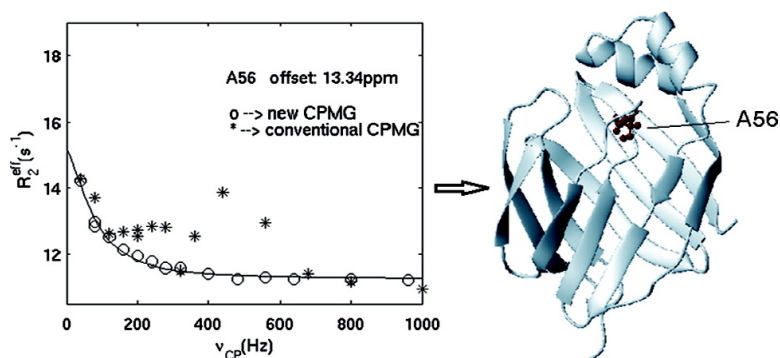# Accurately Probing Slow Motions on Millisecond Timescales with a Robust NMR Relaxation Experiment

Dong Long, Maili Liu, and Daiwen Yang

More About This Article

Additional resources and features associated with this article are available within the HTML version:

- Supporting Information
- Access to high resolution figures
- Links to articles and content related to this article
- Copyright permission to reproduce figures and/or text from this article

View the Full Text HTML

Accurately Probing Slow Motions on Millisecond Timescales with a Robust NMR Relaxation Experiment

Dong Long,[†] Maili Liu,[‡] and Daiwen Yang*,[†]

Department of Biological Sciences, 14 Science Drive 4, National University of Singapore, Singapore 117543, and Wuhan Institute of Physics and Mathematics, Chinese Academy of Sciences, Wuhan, China, 430071

Received November 20, 2007; E-mail: dbsydw@nus.edu.sg

Conformational exchange on micro- to millisecond timescales is an inherent feature of many biochemical events, and NMR is a powerful tool for investigating such dynamic processes.[1] The Carr−Purcell−Meiboom−Gill (CPMG) based relaxation dispersion experiments are one experimental approach to study the exchange processes. The dependence of apparent transverse relaxation rates (R_2^{eff}) on CPMG frequency or field strength (ν_{CP}) can be subsequently used to extract exchange parameters.[2] Efforts have been made to develop experiments for the measurements of single-[3,4] and multiple-quantum[5] relaxation dispersions for amide and methyl moieties in proteins. For the purpose of preserving NMR probes, especially cryoprobes, relatively low radio frequency (rf) field power is normally used during the CPMG pulse trains in the dispersion experiments. In this case, substantial systematic errors may be introduced to the measured relaxation rates due to imperfect refocusing CPMG pulses originating from off-resonance effects, rf inhomogeneity, and miscalibrated pulse parameters, leading to misinterpretation of relaxation data and difficult identification of residues with small exchange contributions to the transverse relaxation (R_{2ex}). A number of methods have been proposed to reduce the systematic errors in the measurement of transverse relaxation time T_2, including applications of adiabatic refocusing pulses,[6] numerical corrections,[7] and uses of phase cycling for the refocusing pulses.[8] The long pulse width of the adiabatic pulses restricts the maximal ν_{CP} value to ∼500 Hz. The numerical correction method requires perfect 180° pulses and homogeneous rf. The phase cycling schemes provide a smaller number of accessible ν_{CP} values than the conventional CPMG.[3,4] Therefore these methods have not been applied to the measurement of relaxation dispersion.

To suppress the systematic errors, the ideal average Hamiltonian during the CPMG trains should be AS_x (AS_y) for an initial magnetization along the x-axis (y-axis), where A denotes average interaction amplitude. Our numerical simulations indicated that the best 4-step phase cycles of the refocusing pulses are (x x y $-y$) and (y y x $-x$) for the initial magnetization along the x-axis and y-axis, respectively (Figure S1 of the Supporting Information). Combining this phase cycling scheme and the conventional scheme, here we describe a pulse scheme for the accurate measurement of relaxation dispersion (Figure 1). To investigate the effects of off-resonance, rf inhomogeneity, scalar coupling, cross-correlated relaxation, and cross relaxation between protons on the evolution of a ${}^{15}N$ spin in an amide group, we performed numerical simulations by assuming a three-spin system, which consists of the ${}^1H$ and ${}^{15}N$ spins in an amide and an effective ${}^1H$ spin. This ${}^1H$ was assumed to be 1.86 Å away from the amide ${}^1H$, representing all the protons proximate to the amide. R_2^{eff} values obtained with the scheme shown in Figure 1 and the conventional CPMG were calculated by solving numerically the quantum mechanical master
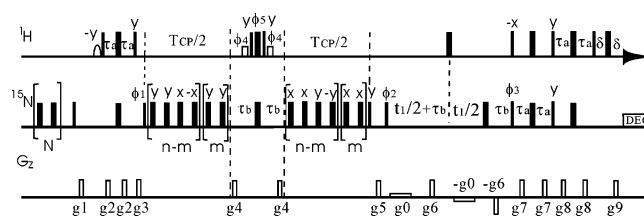
† National University of Singapore.
‡ Chinese Academy of Sciences.

Figure 1. Pulse scheme for the measurement of relaxation dispersion. All narrow (wide) bars represent 90° (180°) rectangular pulses, applied with phase x, unless indicated otherwise. The first shaped ${}^1H$ pulse is a 1.4 ms sinc 90° pulse, while the open rectangles denote 1.6 ms ${}^1H$ 90° pulses. The ${}^{15}N$ pulses before the first 90° pulse and those pulses from pulse ϕ_1 to the point just before pulse ϕ_2 are employed with a field strength of 5.6 kHz, The delays used are $\tau_a = 2.3$ ms, $\tau_b = 2.68$ ms, $\delta = 1.1$ ms, $T_{CP} = 50$ ms $= 2[(n - m)(4\tau_{cp}) + m(2\tau_{cp})]$, where τ_{cp} is the delay between the centers of two successive 180° pulses. $N = 4(1 + n_{max}) - [4(n - m) + 2m]$, where n_{max} is the maximum of $n - m$ and is set to 12. The durations (ms) and strengths (G/cm) of sine-shaped gradients are: g1 = (1, 5), g2 = (1, 15), g3 = (2, 22.5), g4 = (0.5, 20), g5 = (1, −10), g6 = (1, 20), g7 = (1, 25), g8 = (1, 15), g9 = (1, 4.05). Weak bipolar gradients g0 (1.5 G/cm) are used during the t_1 period. The phase cycling used is: $\phi_1 = x, -x$; $\phi_2 = 4(y), 4(-y)$; $\phi_3 = x, -x$; $\phi_4 = 2(x), 2(-x)$; $\phi_5 = 2(-x), 2(x)$; rec = $2(x, -x), 2(-x, x)$.

equation[9] (eq. S1 of the Supporting Information) for each pulse and free evolution period from pulse ϕ_1 to the point just before pulse ϕ_2.

Even when a nearly maximal rf power (rf field strength ν_{1N}^0 of 5.6 kHz) was applied to a cryoprobe during the CPMG, R_2^{eff} obtained with the conventional scheme varied with ν_{CP} more than 1 s^{-1} in the absence of conformational exchange in the cases where nitrogen off-resonance frequencies ($\Delta\omega_N$) were greater than 620 Hz or less than −680 Hz (Figure 2a and Figures S2 and S3 of the Supporting Information). For the scheme shown in Figure 1, by contrast, R_2^{eff} was relatively independent of ν_{CP} (Figure 2b and Figures S3 and S4 of the Supporting Information), and the variation was smaller than 0.5 s^{-1} even when $|\Delta\omega_N|$ was up to 1135 Hz after the measured R_2^{eff} (R_{2exp}^{eff}) values were corrected using the following equation:

$$R_2^{eff} = R_{2\,exp}^{eff} + \frac{(R_2 - R_1)\nu_{CP}(n - m)}{2\nu_{1N}^0(2n - m)} \quad (1)$$

where R_2 and R_1 are the transverse and longitudinal relaxation rates of the ${}^{15}N$ spin in the spin system, respectively; $\nu_{CP} = 1/(2\tau_{cp})$; $n-m$ and m are the numbers of the first and second repetitive elements during one $T_{CP}/2$ period (Figure 1), respectively. The relations between ν_{CP} and n/m are listed in Table S1 of the Supporting Information. The second term in eq 1 corrects the relaxation difference of the magnetization[8b] evolving during the refocusing pulses along the x and y axes in the CPMG sequence.

In the cases where the CPMG rf field deviated from that for a perfect 180° pulse due to rf inhomogeneity and/or pulse miscalibration, R_2^{eff} measured with the conventional CPMG method
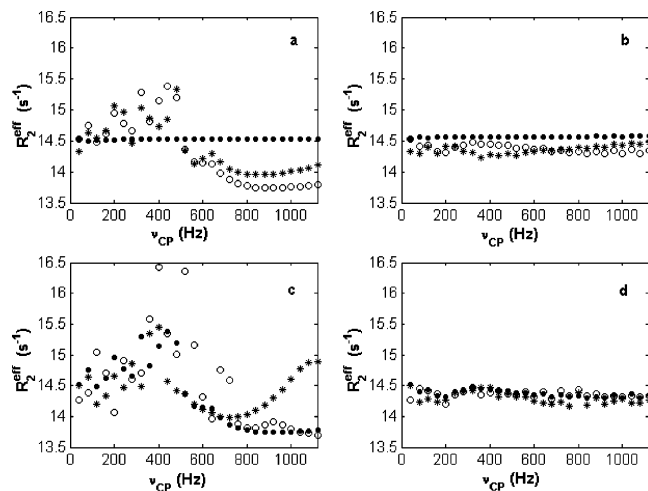
Figure 2. Dependences of ^{15}N R_2^{eff} on ν_{CP} for different $\Delta\omega_N$ and pulse imperfection for two different pulse schemes. The simulated results are shown in panels a and c for the conventional scheme and panels b and d for the scheme shown in Figure 1. Symbols "o", "•", and "∗" in panels a and b denote $\Delta\omega_N$ of +811, 0, and −811 Hz, respectively. Symbols "o", "•", and "∗" in panels c and d denote pulse width deviations from a perfect 180° pulse by +5%, 0, and −5%, respectively, when $\Delta\omega_N = 811$ Hz. The R_2^{eff} values were derived from the relative signal intensity calculated at a T_{CP} value of 50 ms, assuming rf strength of 5.6 kHz, a ^1H frequency of 800 MHz, and an overall tumbling time of 7 ns.

fluctuated with ν_{CP} more significantly (Figure 2c and Figure S5 of the Supporting Information). Moreover, this dependence was asymmetric about a perfect 180° pulse field. On the other hand, the results obtained with the new method were insensitive to the accuracy of the pulse width (Figure 2d and Figure S6 of the Supporting Information). In the absence of CSA-dipole cross-correlated relaxation or/and ^1H-^1H cross-relaxation, the dependences of R_2^{eff} on ν_{CP} were very similar to those in the presence of these relaxation interactions (Figure S7 of the Supporting Information). Thus, the variation of R_2^{eff} with ν_{CP} mainly results from off-resonance effects and rf inhomegeneity.

To test the performance and show the application of the scheme proposed here, we measured the relaxation dispersion profiles of ^{15}N spins for human liver fatty acid binding protein (LFABP) in the absence of fatty acids on a Bruker 800 MHz spectrometer equipped with a cryoprobe. The results obtained with the conventional method and our scheme agreed for the residues with $\Delta\omega_N < 5$ ppm (Figure 3). However, for the residues with larger offsets, the method proposed here produced significantly better results than the conventional one. For residues with small R_{2ex} (e.g., <3 s^{-1}) and large offsets (>700 Hz), we could hardly tell the presence of R_{2ex} from the relaxation dispersion profiles obtained with the conventional CPMG method (Figure 3a). In contrast, regardless of offsets, the data obtained with the new scheme were nearly free of systematic errors. Also, R_2^{eff} values for those residues without conformational exchange were nearly independent of ν_{CP} (Figure 3d and Figure S8 of the Supporting Information). This agrees well with the simulation results.

Human LFABP consists of 127 residues that form a β-barrel, encompassing a ligand binding cavity, and a short helix-turn-helix lid capping one end of the barrel.[10] The interaction between helix II and βC/βD turn determines the opening size of the barrel. Because the structures of the ligand-free and ligand-bound forms are very similar for all FABPs, the mobility of the residues around the lid was considered to be crucial for the entry and exit of fatty acids.[11] We found that most residues in the second helix and all residues in the βC/βD turn in human LFABP displayed conformational exchange on ms timescales. Many residues in βB that follows helix II and most residues in βC and βD showed conformational
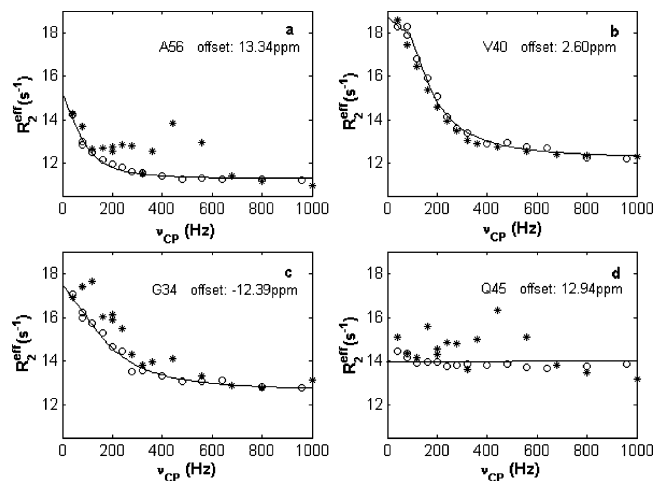

Figure 3. Relaxation dispersion profiles obtained using the new scheme shown in Figure 1 (o) and the conventional scheme (∗). Solid lines are the fitting curves of the experimental data measured with the new scheme to the general equation for a two-state exchange model. The line in panel d is drawn at the average R_2^{eff} values obtained with the new scheme.

exchange. Figure 3 shows a number of residues located in different regions of the protein: G34 in the loop between helix II and βB, V40 in βB, Q45 on the opposite side of the lid (which is expected to have no conformational exchange), A56 in the βC/βD turn. The mobility of LFABP on ms timescales, shown by the relaxation data, could be important for the accommodation of large ligands by LFABP.

In summary, systematic errors in R_2^{eff} can be suppressed significantly with our new scheme. One can reliably map out residues undergoing slow motions and further extract more accurate kinetics parameters with the experiment shown here.

Supporting Information Available: Seven figures showing the dependences of R_2^{eff} on ν_{CP}, $\Delta\omega_N$, and rf fields, one showing the average Hamiltonian for two phase cycling schemes, one table listing the relations between ν_{CP} and n/m. This material is available free of charge via the Internet at http://pubs.acs.org.

References

(1) Mittermaier, A.; Kay, L. E. *Science* **2006**, *312*, 224−8.
(2) Palmer, A. G.; Kroenke, C. D.; Loria, J. P. *Methods Enzymol.* **2001**, *339*, 204−38.
(3) (a) Loria, J. P.; Rance, M.; Palmer, A. G. *J. Am. Chem. Soc.* **1999**, *121*, 2331−32. (b) Mulder, F. A. A.; Skrynnikov, N. R.; Hon, B.; Dahlquist, F. W.; Kay, L. E. *J. Am. Chem. Soc.*, **2001**, *123*, 967−75. (c) Skrynnikov N. R.; Mulder, F. A. A.; Hon, B.; Dahlquist, F. W.; Kay, L. E., *J. Am. Chem. Soc.*, **2001**, *123*, 4556−66. (d) Ishima, R.; Torchia, D. A. *J. Biomol. NMR* **2003**, *25*, 243−48.
(4) Tollinger, M.; Skrynnikov, N. R.; Mulder, F. A. A.; Forman-Kay, J. D.; Kay, L. E. *J. Am. Chem. Soc.* **2001**, *123*, 11341−52.
(5) Orekhov, V. Y.; Korzhnev, D. M.; Kay, L. E. *J. Am. Chem. Soc.* **2004**, *126*, 1886−91.
(6) Zweckstetter, M.; Holak, T. A. *J. Magn. Reson.* **1998**, *133*, 134−47.
(7) Korzhnev, D. M.; Tischenko, E. V.; Arseniev, A. S. *J. Biomol. NMR* **2000**, *17*, 231−37.
(8) (a) Gullion, T.; Baker, D. B.; Conradi, M. S. *J. Magn. Reson.* **1990**, *89*, 479−84. (b) Yip, G. N. B.; Zuiderweg, E. R. P. *J. Magn. Reson.* **2004**, *171*, 25−36.
(9) Ernst, R. R.; Bodenhausen, G.; Wokaun, A. *Principles of Nuclear Magnetic Resonance in One and Two Dimensions;* Oxford University Press: Oxford, U.K., 1987.
(10) Hamilton, J. A. *Prog. Lipid Res.* **2004**, *43*, 177−99.
(11) Hodsdon, M. E.; Cistola, D. P. *Biochemistry* **1997**, *36*, 2278−90.

JA710477H